

# Dual-Tree Wavelet Transform for Medical Image Watermarking



Romain Mavudila Kongo<sup>1</sup>, Lhousaine MASMOUDI<sup>1</sup>, Mohammed CHERKAOUI<sup>2</sup>, Ahmed ROUKHE<sup>3</sup>

<sup>1</sup>Nadia Idrissi, Najem HASSANAIN  
LETS Laboratory, Physics Department  
Mohamed V University  
Rabat, Morocco

<sup>2</sup>Faculty of Medicine and pharmacy  
Fès, Morocco

<sup>3</sup>Faculty of sciences, Meknes. Morocco

**ABSTRACT:** Wavelet techniques can be successfully applied in various image processing methods, namely in image denoising, segmentation, classification, watermarking and others. Given the earlier works of watermarking images based on DT-CWT, our approach shown that it is possible to generalize their conclusions and to show some results in the medical watermarking images. It has been demonstrated in the literature that the Complex Wavelet Transform (DT-CWT), has significant advantages over classic Discrete Wavelet Transform (DWT), for certain image processing problems. The DT-CWT is a form of Discrete Wavelet Transform which generates complex coefficients by using a dual tree of wavelet filters to obtain their real and imaginary parts. The main part of the paper is devoted to exploit the exceptional quality of DT-CWT combined with Bivariate Shrinkage with Local Variance Estimation at the extracted step of the watermark in the blind watermarking of medical images. The results of simulation showed that DT-CWT gave better quality of watermarked images and preserved a integrity of image after extracting watermark. We suggested that the findings obtained by this study will help to uncover in medical watermarking images and seemed to reaffirm the findings of previous researches in robustness and traceability and transparency preservation.

**Keywords:** Complex Wavelet Transform, Image Watermarking, Bivariate Shrinkage, Medical Image Security

**Received:** 23 March 2012, Revised 10 June 2012, Accepted 19 June 2012

© 2012 DLINE. All rights reserved

## 1. Introduction

Medical image protection and authentic are becoming increasingly important in an e-health environment where images are readily distributed over electronic networks. Research has shown that medical image watermarking is a relevant process for enhancing data security, content verification and the image fidelity.

At the same time, it is necessary to preserve as much original information in the image data as possible, to avoid causing performance loss for human viewers. Most medical image watermarking research focuses on developing watermarking systems that preserve image fidelity and/or robustness, under typical non-medical image degradation processes. Cryptography was first technique proposed for digital document security; however, once decrypted, the document is no longer protected and can be distributed dishonestly unprotected. Watermarking combine the proprieties of steganography and cryptography [1].

In general, we can insert the watermark in the spatial domain or the transform domain, the first domain, embedding the data by modify the pixel values of the host image directly, are susceptible to simple image operation such as randomizing the Least Significant Bit (LSB),cropping and loss compression and the second, the watermarking scheme is in transform domain, such as Discrete Fourier transform (DFT); Discrete transform Cosine (DCT) and Discrete Wavelet Transform (DWT), provide more advantages and better performances than those in spatial domain in the most recent researches [2]. Various methods have been developed in the literature in medical image watermarking , most of them used only the standard wavelet transform (DWT).

However, the Discrete Wavelet Transform (DWT) has limits and some disadvantages that undermines its application in image processing [3].

In this study we wanted to exploit the exceptional quality of DT-CWT combined with Bivariate Shrinkage for medical image watermarking, method capable of giving us back an exact duplicate of the original image, critical criterion of reversibility in the medical field.

## 2. Wavelet Transform Approach

### 2.1 Discrete Wavelet Transform (DWT)

The implementation of an analysis filterbank for a single level 2-D DWT shown in Figure 1, with the algorithm of Mallat on the decomposition of an image, with two filter banks, low pass and high pass, respectively .

This structure produces detailed sub-images ( $D_j(1)$ ,  $D_j(2)$  and  $D_j(1)$ ) corresponding to three different directional-orientation (horizontal ,vertical and diagonal) and a lower resolution sub-image  $A_j$  [4].

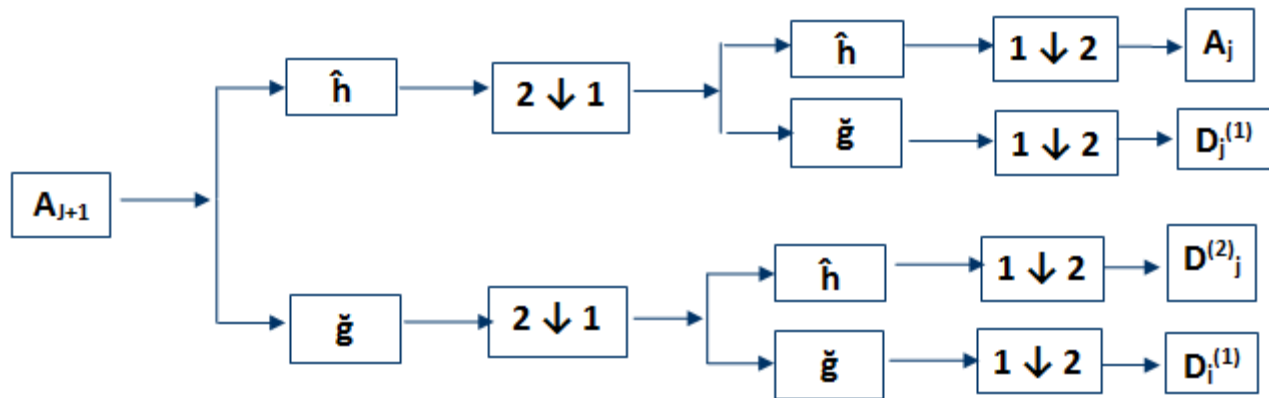


Figure 1. Mallat's algorithm diagram for wavelet decomposition of an image

The  $A_{j+1}$  image is decomposed via DWT or DT-CWT .

The filter bank structure can be iterated in a similar manner on  $A_j$  channel to provide multilevel decomposition, as illustrated in Figure 2.

The classical discrete wavelet transform (DWT) provides a means of implementing a multiscale analysis, based on a critically sampled filter bank with perfect reconstruction [21].

### 2.2 Limits of the discrete wavelet transform (DWT)

However, questions arise regarding the good qualities or properties of the wavelets and the results obtained using these tools, the standard DWT suffers from the following problems described as below:

- Shift sensitivity: it has been observed that DWT is seriously disadvantaged by the shift sensitivity that arises from down samples in the DWT implementation [3, 5].
- Poor directionality: an m-dimension transform ( $m > 1$ ) suffers poor directionality when the transform coefficients reveal only a few feature in the spatial domain.

– absence of phase information: filtering the image with DWT increases its size and adds phase distortions; human visual system is sensitive to phase distortion [6]. Such DWT implementations cannot provide the local phase information.

In other applications, and for certain types of images, it is necessary to think of other, more complex wavelets, who gives a good way, because the complex wavelets filters which can be made to suppress negative frequency components . As we shall see the CWT has improved shift-invariance and directional selectivity [7].

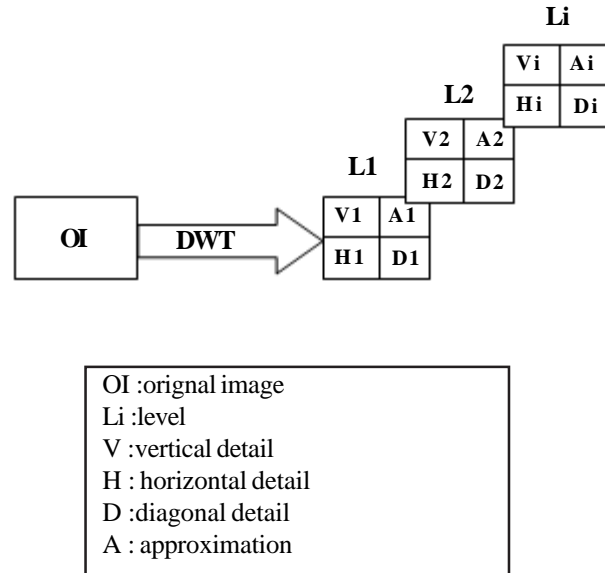


Figure 2. Multilevel decomposition hierarchy of image with DWT

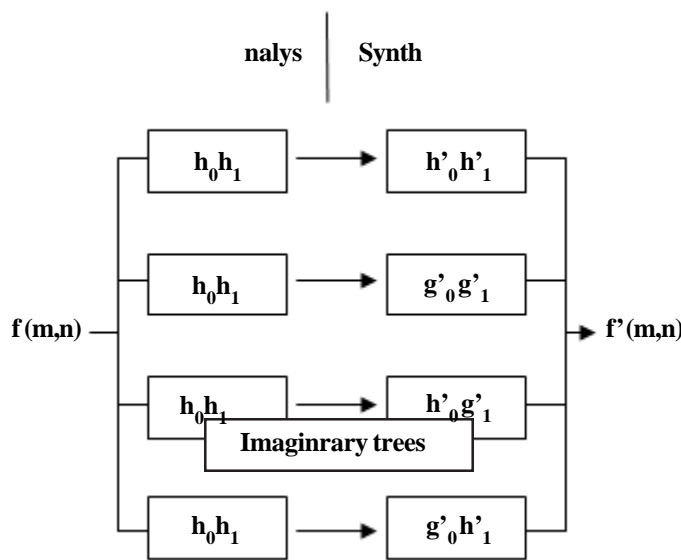


Figure 3. Filterbank structure for DT-DWT

## 2.2 Complex Wavelet Transform (CWT)

Complex wavelet transform use complex valued filtering (analytic filter) that decomposes the real/complex signal into real and imaginary parts in transform domain. The real and imaginary coefficients are used to compute amplitude and phase information, just the type of information needed to accurately describe the energy localization of oscillating functions (wavelet basis).

### 2.2.1 Dual-tree wavelet Transform (DT-DWT)

The discrete and complex dual tree wavelet transform (DTCWT) was introduced by N. Kingsburg around 1990.

This implementation uses consists in analyzing the signal by two different DWT trees, with filters chosen so that at the end, the signal returns with the approximate decomposition by an analytical wavelet.

The dual-tree structure has an extension of conjugate filtering in 2-D case, this structure is shown in Figure 3.

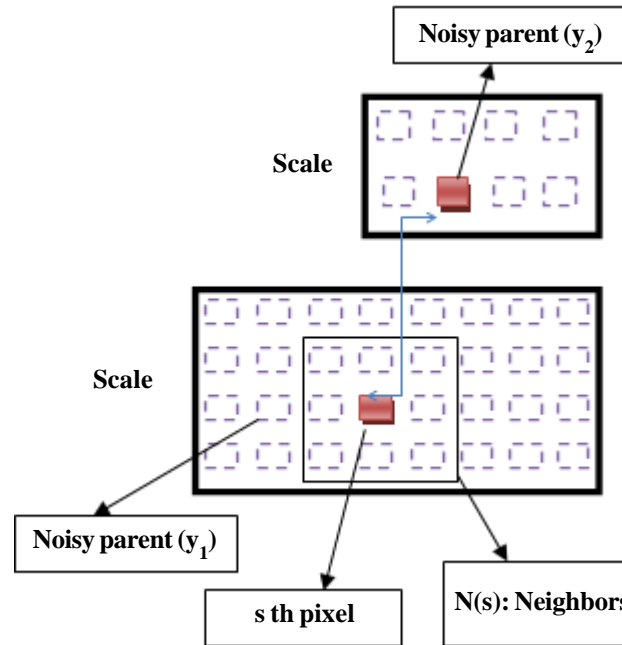


Figure 4. Dependency across scales of wavelet coefficients (neighborhood  $N(K)$  illustration)

This structure needs four trees for analysis as well as for synthesis. The pairs of conjugate filters are applied to two dimensions (0 and 1), which can be expressed as :

$$(h_0 + jg_0)(h_1 + jg_1) = (h_0h_1 - g_0g_1) + j(h_0g_1 + g_0h_1) \quad (10)$$

The synthesis of filters suitable for this structure was performed by several people.

In particular, Kingsbury proposed the use of a type of filters called Qshift, which we did not use in our study.

The wavelet corresponding to the tree's "imaginary part" is very close to the Hilbert transform of the wavelet corresponding to the tree's "real part" [8].

In comparison with DWT, DT-DWT improved directionality with more orientations suggests the advantages in a wide range of directional image.

The DT-CWT ensures filtering of the results without distortion and with a good ability for the localization function and the perfect reconstruction (PR) of signal .

To obtain uniform intervals between samples of the two trees, the filters in one tree must provide delays that are half a sample different from those in the tree in front. For the linear phase, the length of the odd filter in a tree must be the same as the even filter.

In the noise study, as with any redundant frame analysis, when a stationary noise, even if white, is subject to a dual decomposition tree, statistical dependencies appear between coefficients [5, 6, 8], because of the existence of two trees, it appears that the second noise coefficients moments from such decomposition can be precisely characterized.

We observe a decorrelation between primal and dual coefficients located at the same spatial position and an inter-scale correlation, which allows us to choose between several estimators, taking this phenomenon into account.

If we consider an image  $S$  degraded by a Gaussian  $n$ , white, centered, additive Gaussian noise with a spectral density, the decomposition coefficients are also affected by that same noise as part of the linearity property.

The noise spectral density can be known or not, we can use a robust estimator calculated from the coefficients of the higher frequency bands [7,9,10].

With this advantage we can choosing a appropriate estimator for denoising and the case of DT-DWT, we will estimate the spectral density in each tree.

### 3. The Bivariate MAP Estimator

Implemented by Levent Sendur and Ivan W. Selesnick [22], gives a performance for image denoising, exploiting the statistical dependence between wavelet coefficients and their ‘parents’.

In considering than image as corrupted by additive independent white Gaussian noise with variance  $\sigma_b^2$

In the multiresolution domain, if we use the orthogonal wavelet transform, the denoising problem can be formulated as follows:

$$y = w + b \tag{11}$$

$y$  being the noise coefficient,  $w$ , the original coefficient, and  $b$ , corresponding to the Gaussian independent noise. Our goal is to estimate  $w$  from  $y$ . To do this, we will use an MPE (Maximum Posterior Estimator) filter [11].

Let  $w_{2\eta}$  represent the “parent” of  $w_{1\eta}$ ; where  $w_{2\eta}$  is the wavelet coefficient at the same position as the  $K$ th wavelet coefficient  $w_{1\eta}$ , but at the next coarser scale .

In wavelet domain the problem have been formulated as follow:

$$y_{1\eta} = w_{1\eta} + b_{1\eta} \text{ and } y_{2\eta} = w_{2\eta} + b_{2\eta} \tag{12}$$

Where ;  $y_\eta = (y_{1\eta} + y_{2\eta})$  noisy coefficient (child and parent),  $w_\eta = (w_{1\eta} + w_{2\eta})$ : original coefficients and  $b_\eta = (b_{1\eta} + b_{2\eta})$  Gaussian independent noise .

If the  $y_1$  coefficient is the considered an detail and  $y_2$  is considered its “parent” (the detail coefficient located in the same geometric position, but calculated in the next iteration. Each sub-band “parent” coefficient will be over-sampled for the same number of elements than that of the corresponding “children” coefficients shown in Figure 4.

The standard MAP estimator for  $\omega$  given the corrupted observation  $y$  is :

$$\hat{w}(y) = \operatorname{argmax}_w [\ln (P_b(y_\eta - w_\eta) P_{w_\eta}(w_\eta))] \tag{13}$$

In considering than image as corrupted by additive white Gaussian noise with zero mean we can write:

$$P_b(b_\eta) = \frac{1}{2\pi\sigma_b^2} e^{-\frac{b_{1\eta}^2 + b_{2\eta}^2}{2\sigma_b^2}} \tag{14}$$

Using the notation as:

$$f(w_\eta) \ln P_{w_\eta}(w_\eta) \tag{15}$$

Proposed in [34] the model for useful image in wavelet transform as:

$$P_{w_\eta}(w_\eta) = \frac{2}{2\pi\sigma^2} e^{-\frac{\sqrt{3}}{\sigma} \sqrt{(w_{1\eta}^2 + w_{2\eta}^2)}} \tag{16}$$

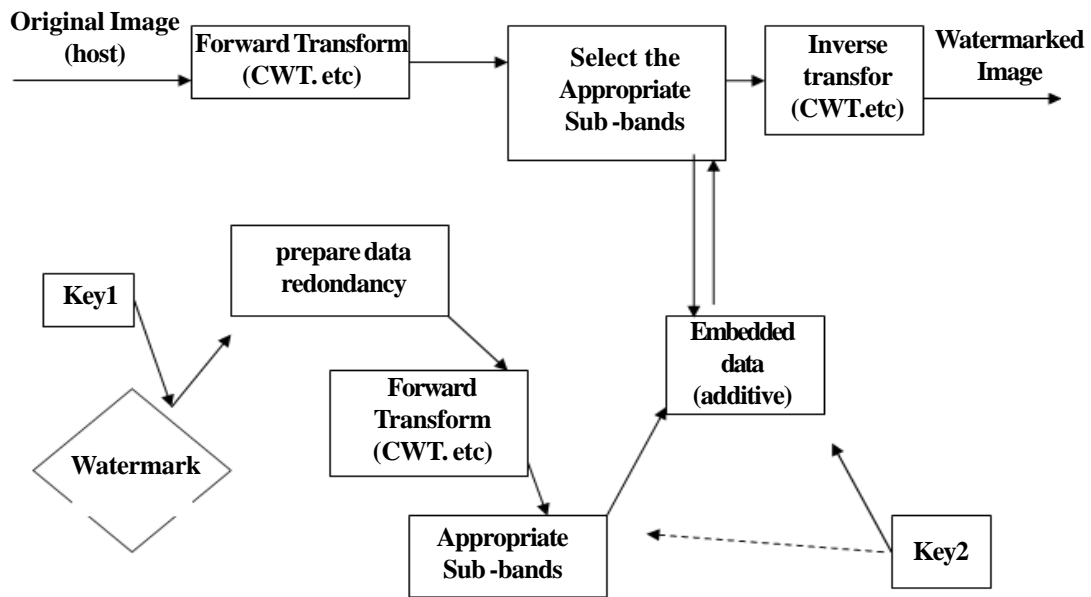


Figure 5. Watermarking embedding scheme

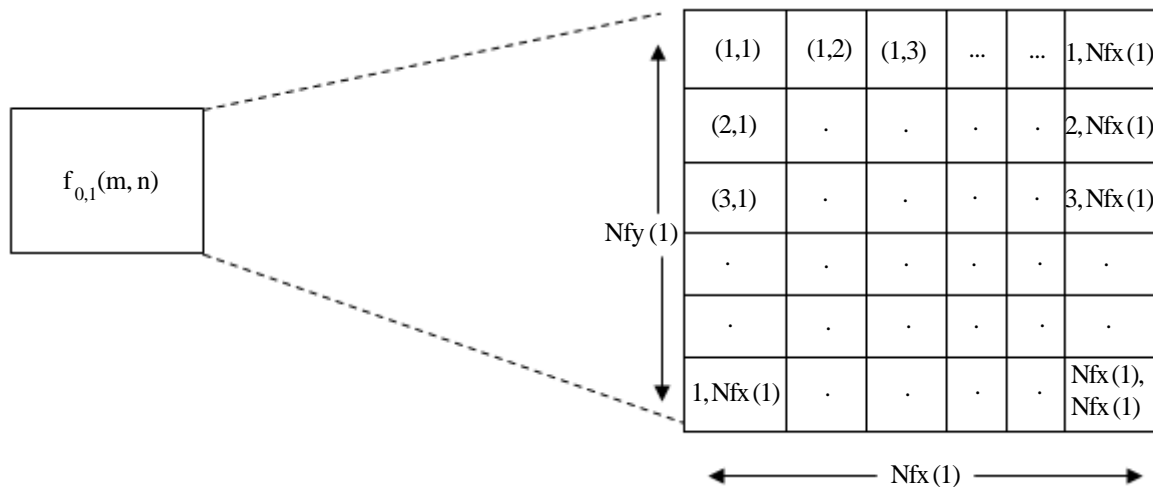


Figure 6. l'indexation spatiale de pixels de coefficients pour l et o donnés, commence par (1,1) et fini par Nfx(1),Nfy(1)

Where,  $w_\eta$  represents the set of coefficients on the  $\eta^{\text{th}}$  of wavelet transform of useful image calculated to  $\eta^{\text{th}}$  iteration and  $w_{2\eta}$  is the set of coefficients of the useful image calculated to the next iteration.

The equation of the MAP filter defined in (14) and (15) takes the form defined in :

$$\hat{w}(y) = \underset{w_\pi}{\operatorname{argmax}} \left\{ -\frac{(y_{1\eta} - w_{2\eta})^2 - (y_{2\eta} - w_{2\eta})^2}{2\sigma_b^2} + f(w_\eta) \right\} \quad (17)$$

This form is equivalent to the equation system:

$$\frac{(y_{1\eta} - w_{2\eta})^2}{\sigma_b^2} + \frac{\alpha f(w_\eta)}{2w_\eta} = 0 \quad (18)$$

i.e :

$$\frac{(y_{2\eta} - w_{2\eta})^2}{\sigma_b^2} + \frac{\alpha f(w_\eta)}{2w_\eta} = 0$$

$$\frac{(y_{1\eta} - w_{1\eta})^2}{\sigma_b^2} + f_1(w_\eta) = 0 \tag{19}$$

$$\frac{(y_{2\eta} - w_{2\eta})^2}{\sigma_b^2} + f_2(w_\eta) = 0$$

Considering the definition of the function f, we can write :

$$f_1(w_\eta) = \ln P_w(w_\eta) \tag{20}$$

Taking into account the density of probability expressed in (14), the system of equation the form as:

$$\frac{(w_{1\eta} - y_{1\eta})^2}{\sigma_b^2} + \frac{\sqrt{3}}{\sigma} \frac{\overline{w_{1\eta}}}{\sqrt{(w_{1\eta}^2 + w_{2\eta}^2)}} = 0 \tag{21}$$

$$\frac{(w_{2\eta} - y_{2\eta})^2}{\sigma_b^2} + \frac{\sqrt{3}}{\sigma} \frac{\overline{w_{2\eta}}}{\sqrt{(w_{1\eta}^2 + w_{2\eta}^2)}} = 0$$

The nth solution of the last equations system is as follows:

$$\hat{w}_{1\eta} = \frac{[\sqrt{(x_1^2 + y_2^2)} - \frac{\sqrt{3}\sigma_\eta^2}{\sigma}]^+}{\sqrt{(x_1^2 + y_2^2)}} \cdot y_{1\eta} \tag{22}$$

Which can be interpreted as a bivariate shrinkage function. Here  $(g)^+$  is defined as:

$$(g)^+ = \begin{cases} 1, & \text{sig} < 0 \\ 0, & \text{otherwise} \end{cases} \tag{23}$$

The marginal variance  $\sigma^2$  is also dependent on the coefficient index  $\eta$  and sigma for  $\eta$ th coefficient will be estimated using neighboring coefficient the region  $N(\eta)$ ; where  $N(\eta)$  is defined as all coefficients within a square shaped window that in centered at the  $\eta$ th coefficient. Figure 3 [33].

The noise variance  $\sigma_b^2$  is estimated from the robust median estimator as follow:

$$\hat{\sigma}_b^2 = \frac{\text{median}(|y_i|)}{0.6745} \cdot y_i \in \text{sous - band HH} \tag{24}$$

From this observation model, one gets;

$$\sigma^2 = \sigma_\eta^2 - \sigma_b^2 \tag{25}$$

where .....is the marginal variance of noisy observations  $y_1$  and  $y_2$ . Since  $y_1$  and  $y_2$  are modeled as zero mean, .... Can be found empirically by:

$$\hat{\sigma}_\eta^2 = \frac{1}{M} \sum_{y_i \in N(\eta)} y_i^2 \tag{26}$$

M; is the size of the neighborhood  $N(\eta)$ , than ... can be estimated as :

$$\hat{\sigma} = \sqrt{(\hat{\sigma}_\eta^2 - \hat{\sigma}_b^2)} \tag{27}$$

#### 4. Previous work

In this paragraph, an overview of the important existing watermarking schemes based also wavelet transform in medical domain and others.

W. Puech and al[12] proposed a watermarking scheme for encrypted the image, developing interfaces for viewing medicals by combining with encryption techniques; a system enables secure medical images by generating a key for encrypting the image. In the latter and companion works, watermarking images with wavelet transform are developed in parallel which addresses the problems of medical confidentiality protection and both origin and data authentication, only with the classical wavelet (DWT) ,[13], [14], [15], [16] and [17].

The watermarking algorithm have been presented in Complex wavelet domain [18, 19],without medical domain.

#### 5. Proposed Experimental Method

As Carified earlier, most of the previous wavelet based watermarking techniques different parts of the image in the same way.

Considering the watermark is a pseudo randomly generated noise, we suggested the following watermarking scheme:

Space watermarked associated with this method is composed of six sub bands of finer details of CWT of image, of size  $(2m, 2n)$  selected. We will proceed in five steps for the implementation of our process and the Figure 4. below is illustrating the first part containing the tree early steps:

##### Step 1. Embedding stage

- We compute a wavelet transform, in the image  $f$  of size  $(2m, 2n)$  and watermark image.
- We select the appropriate sub-band  $f_{o,l}(m, n)$ , with  $l = 1, 2, \dots, L$ , who is resolution level and  $o = 1, 2, 3, \dots, 6$  represents the frequency orientation, corresponding to the sub bands under consideration image  $f$ , and finally  $(m, n)$ , is the particular spatial index at the resolution level  $l$ . (Figure 6).

##### Key generation

As schematically in Figure 5 before decomposed with Wavelet transform, the mark is is managed with a key1, by repetition (redundancy or not) for flexible robustness .

The watermark data are embedded in coefficients wavelet by another secret key2, using the following function:

$$f_{w o,l}(m, n) = f_{o,l}(m, n) + [1 + k * W_{0,l}(m, n)]. \quad (28)$$

where  $f_{w o,l}(m, n)$  and  $f_{o,l}(m, n)$  are a singular value of oth sub-band of watermarked original images and  $W_{0,l}(m, n)$  shows the singular value of the oth watermark sub-band; and  $k$  is a parameter characterizing the strength of watermarking. For the empirical experience  $k = 0.2$  are chosen to balance the trade-off between fidelity and robustness.

- We denote that each sub-image  $f_{o,l}(m,n)$  is composed of pixels representing values coefficients for the variables  $(m,n)$ , and this spatial location is indexed  $(1,1)$  to  $(N_{fx}(l), N_{fy}(l))$ .
- in which Redundancy comes into our patterns of integration or retrieval of the mark, by the fact that the size of the mark needed to identify without ambiguity is the order of a few bytes, or one image is a volume of binary information well higher, the key1 has be used to prepare it.
- The constructing stage corresponds to the inverse wavelet transform , applied to the coefficients wavelet, for,  $\sum f_{w o,l}(m,n)$  at different levels resolution and the watermarked image  $f_w$ , will be constructed, by the following equation:

$$f_w = ICWT [\sum f_{w o,l}(m, n)] \quad (29)$$

##### Step 2. Extraction stage

The diagram of the extraction procedure is shown in Figure 7, watermark  $W$  had be extracted without host image , only with the



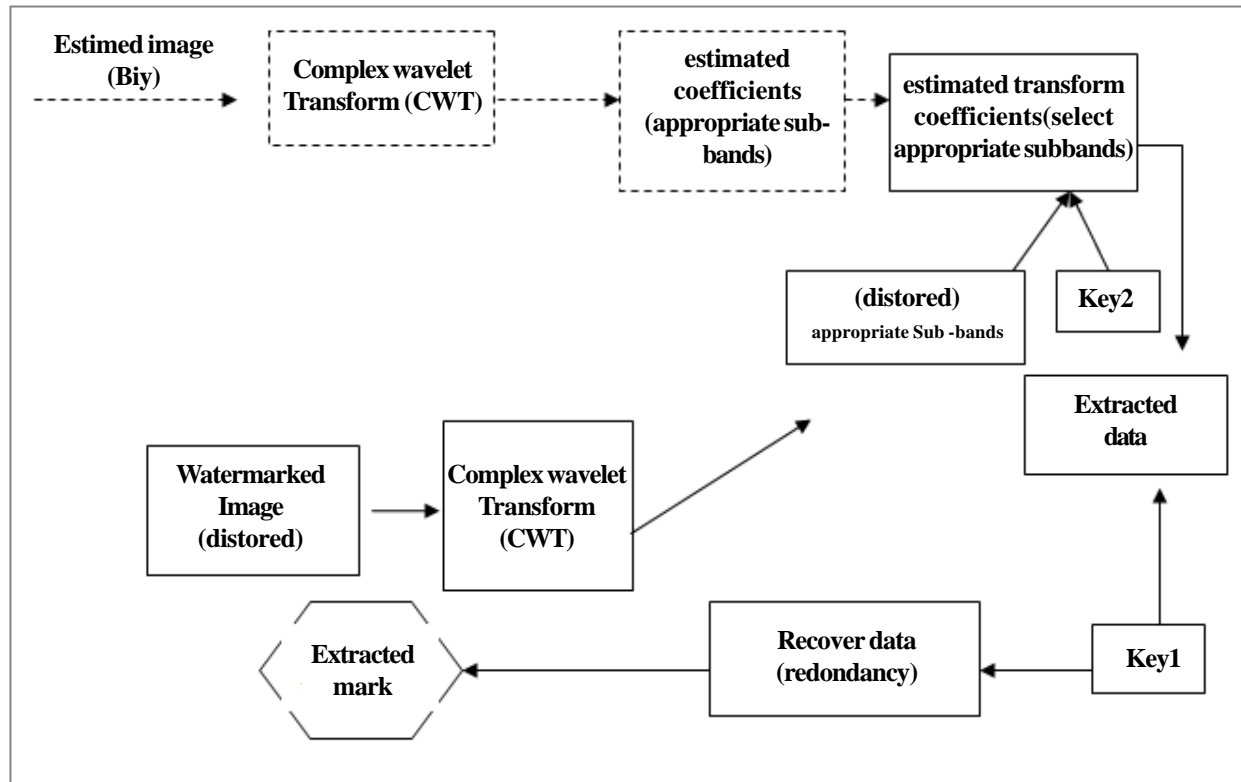


Figure 7. Diagram of the extraction procedure

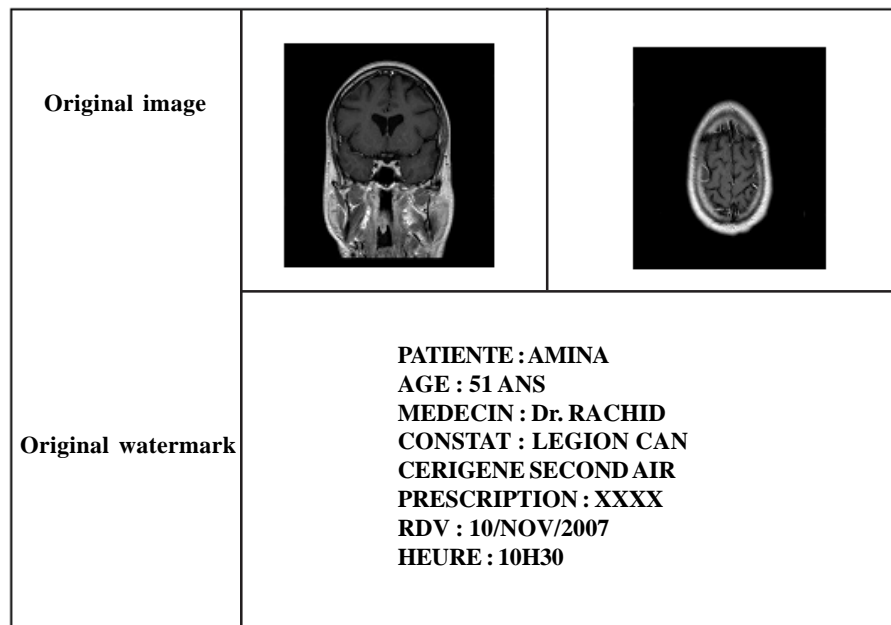


Figure 8. Original Coronal and Axial images and original watermark

same secret key2 used for the incorporation of the watermark and watermarked image.

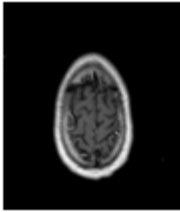
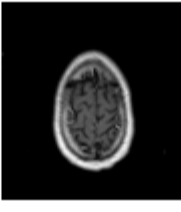
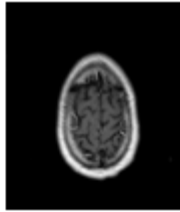
watermarked image are esteemed with the following rule:

- Let  $Y = \text{CWT}(J)$  and  $Y' = \text{CWT}(fw)$ , where  $J$  is the estimated image, with Bivariate Shrinkage and  $fw$  the watermarked image.

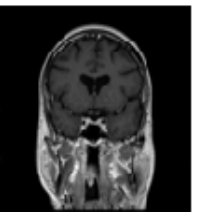
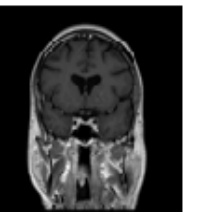
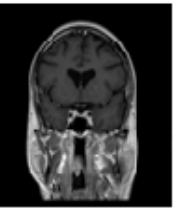
- The coefficients of the watermark are found with the difference between each select coefficient of the appropriate sub-band of Y and each select coefficient of the appropriate sub-band of Y', as follow equation:

$$t_{o,l}(m, n) = [(f_{w o, l}(m, n) - J_{o,l}(m, n))] / k \quad (30)$$

- and we sum the differences for obtain the extracted data of watermark t.

<b>JPEG Compression Watermarked Image</b>			
<b>Detected Watermark Image</b>	<b>PATIENTE : AMINA</b> <b>AGE : 51 ANS</b> <b>MEDECIN : Dr. RACHID</b> <b>CONSTAT : LEGION CAN</b> <b>CERIGENE SECONDAIR</b> <b>PRESCRIPTION : XXXX</b> <b>RDV : 10/NOV/2007</b> <b>HEURE : 10H30</b>	<b>PATIENTE : AMINA</b> <b>AGE : 51 ANS</b> <b>MEDECIN : Dr. RACHID</b> <b>CONSTAT : LEGION CAN</b> <b>CERIGENE SECONDAIR</b> <b>PRESCRIPTION : XXXX</b> <b>RDV : 10/NOV/2007</b> <b>HEURE : 10H30</b>	<b>PATIENTE : AMINA</b> <b>AGE : 51 ANS</b> <b>MEDECIN : Dr. RACHID</b> <b>CONSTAT : LEGION CAN</b> <b>CERIGENE SECONDAIR</b> <b>PRESCRIPTION : XXXX</b> <b>RDV : 10/NOV/2007</b> <b>HEURE : 10H30</b>

**A**

<b>JPEG Compression Watermarked Image</b>			
<b>Detected Watermark Image</b>	<b>PATIENTE : AMINA</b> <b>AGE : 51 ANS</b> <b>MEDECIN : Dr. RACHID</b> <b>CONSTAT : LEGION CAN</b> <b>CERIGENE SECONDAIR</b> <b>PRESCRIPTION : XXXX</b> <b>RDV : 10/NOV/2007</b> <b>HEURE : 10H30</b>	<b>PATIENTE : AMINA</b> <b>AGE : 51 ANS</b> <b>MEDECIN : Dr. RACHID</b> <b>CONSTAT : LEGION CAN</b> <b>CERIGENE SECONDAIR</b> <b>PRESCRIPTION : XXXX</b> <b>RDV : 10/NOV/2007</b> <b>HEURE : 10H30</b>	<b>PATIENTE : AMINA</b> <b>AGE : 51 ANS</b> <b>MEDECIN : Dr. RACHID</b> <b>CONSTAT : LEGION CAN</b> <b>CERIGENE SECONDAIR</b> <b>PRESCRIPTION : XXXX</b> <b>RDV : 10/NOV/2007</b> <b>HEURE : 10H30</b>

**B**

Figure 9. Watermaked Axial(A) and coronal (B) images and its extract watermark (Jpeg attack)

**Performance of Method**

The performance of the proposed approach is measured in one side by the quantitative measures namely MSE (mean square Error) and PSNR (peak Signal to Noise ration) between host and restored images are determined as :

$$MSE = \frac{1}{MN} \sum_{i=1}^M \sum_{j=1}^N (X(i, j)) \tag{31}$$

And,

$$PSNR (dB) = 10 \log_{10} (255^2 / MSE) \tag{32}$$

However, robustness is measured by similarity (Sim.) given by the follow equation:

$$Sim (t, W) = \sum_i \sum_j (t(i, j).W(i, j)) / \sum_i \sum_j (W^2(i, j)); \tag{33}$$

where t (i, j) and W(i, j) are respectively value of original and extracted watermark [20, 21].

Mathematic measures used have some limits for to affirm the performances for our approach, a test has been increased to radiologists address on the quality of images; this test methodology is as follows:

Considering the brain images of two sequences commonly used in MRI, Axial and Coronal. These images were watermarked with forward wavelet transforms. The images were anonymized (de-identifier) first-time summers and radiologists were asked the question, whether the image presented to it is original or watermarked and if it is acceptable to the diagnosis and answer yes or no.

Secondly watermarked image compared to the image host for each case placed side by side, this time the original is revealed , the observer will quantify on scale of 1-9 shown:

1: Inacceptable pour le diagnostic; 9: No visible difference; 7: No loss of diagnostic information; 5: In the limit of loss information, discrete anomalies can be omitted; 3: Important diagnostic information can be omitted, degradation affects the interpretation and 1: unsatisfactory for diagnosis indisputable loss of diagnostic information.

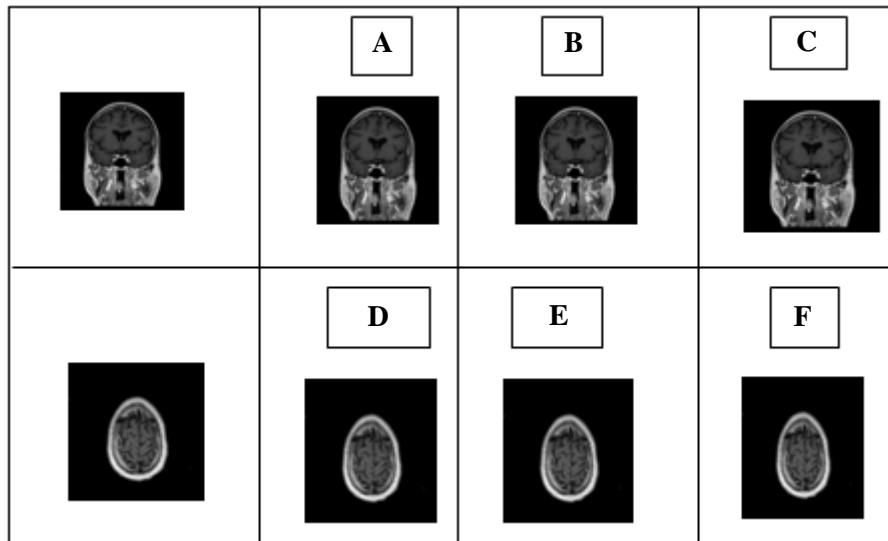
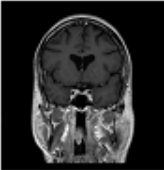
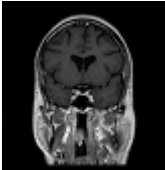
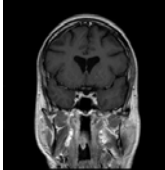


Figure 10. at left ,above and below ;original images and, A, B, C, D, E, F Watermarked images with CWT, Real DWT and DWT

**6. Results and Discussion**

The watermark used in this study was (logo image), which has two important advantages:

- the extracted image watermark can be correlated with the host image mark to a human observer, the existence of a visual logo in the image, was evidence of statistical correlation value.

<b>JPEG Compression Watermarked Image</b>	<b>Noised image</b> 	<b>Noised image</b> 	<b>Noised image</b> 
	<b>Detected Watermark Image</b>	<b>Detected Watermark Image</b>	<b>Detected Watermark Image</b>
	PATIENTE : AMINA AGE : 51 ANS MEDECIN : Dr. RACHID CONSTAT : LEGION CAN CERIGENE SECONDAIR PRESCRIPTION : XXXX RDV : 10/NOV/2007 HEURE : 10H30	PATIENTE : AMINA AGE : 51 ANS MEDECIN : Dr. RACHID CONSTAT : LEGION CAN CERIGENE SECONDAIR PRESCRIPTION : XXXX RDV : 10/NOV/2007 HEURE : 10H30	PATIENTE : AMINA AGE : 51 ANS MEDECIN : Dr. RACHID CONSTAT : LEGION CAN CERIGENE SECONDAIR PRESCRIPTION : XXXX RDV : 10/NOV/2007 HEURE : 10H30

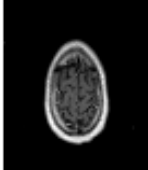
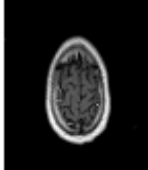
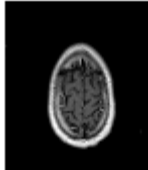
<b>JPEG Compression Watermarked Image</b>	<b>Noised image</b> 	<b>Noised image</b> 	<b>Noised image</b> 
	<b>Detected Watermark Image</b>	<b>Detected Watermark Image</b>	<b>Detected Watermark Image</b>
	PATIENTE : AMINA AGE : 51 ANS MEDECIN : Dr. RACHID CONSTAT : LEGION CAN CERIGENE SECONDAIR PRESCRIPTION : XXXX RDV : 10/NOV/2007 HEURE : 10H30	PATIENTE : AMINA AGE : 51 ANS MEDECIN : Dr. RACHID CONSTAT : LEGION CAN CERIGENE SECONDAIR PRESCRIPTION : XXXX RDV : 10/NOV/2007 HEURE : 10H30	PATIENTE : AMINA AGE : 51 ANS MEDECIN : Dr. RACHID CONSTAT : LEGION CAN CERIGENE SECONDAIR PRESCRIPTION : XXXX RDV : 10/NOV/2007 HEURE : 10H30

Figure 11. Test image under JPEG compression attack (DWT, R.DWT and CWT)

We have below the original images and the watermark For the decomposition of the image, we used, three transformed wavelet; DWT, real DWT and CWT, the results of watermarking are presented as following:

Figure 9 shown the watermaed images Axial and coronal and its extract watermark version without attack.

The PSNRs values between these each images are presented in table1.

There is no visual difference between original and watermarked images for each case which satisfy the strictest requirement of medical image watermarking. Each medical images was subject to different attacks, tables 2 and 3, shown the PSNR.

Whatever the method of wavelet decomposition chosen, we cannot that poorer performances was achieved with DWT, and also in all tests; DWT, real DWT, CWT.

The results obtained are summarized in the Tables 2 and 3, numbers in bold in each column indicate the highest PSNRs

correspond generally to the CWT. Analysis of results shows, ours proposed scheme has high degree of robustness to sharpen and JPEG attacks specially for CWT followed by real DWT for each case.

The information of watermark can be recovered without any error, and similarity between recovered and original information is equal to 0.9989 for the two types of images as shown in table 2 and 3.

In addition, JPEG with quality factor 90% , 70% gives, best result for each case, if we go down to 60%, 50%, we obtained the poor results for DWT for each case.

An observing the images attacked by sharpen and median filter only with DWT, watermark data are visible in back-round, the reason is that we wanted to experiment parameter k characterizing the strength of watermarking with the value superior ( $k = 0.5$ ).

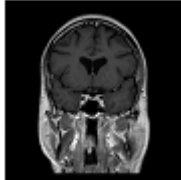
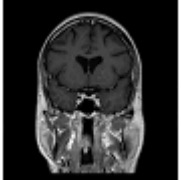
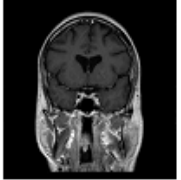
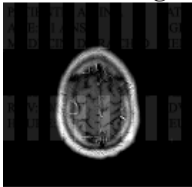
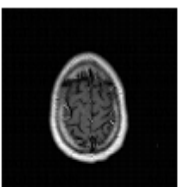
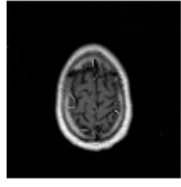
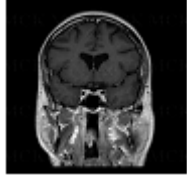
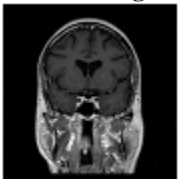
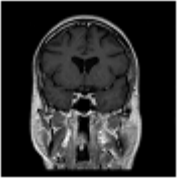
<b>JPEG Compression Watermarked Image</b>	<b>Noised image</b> 	<b>Noised image</b> 	<b>Noised image</b> 
	<b>Detected Watermark Image</b>	PATIENTE : AMINA AGE : 51 ANS MEDECIN : Dr. RACHID CONSTAT : LEGION CAN CERIGENE SECONDAIR PRESCRIPTION : XXXX RDV : 10/NOV/2007 HEURE : 10H30	PATIENTE : AMINA AGE : 51 ANS MEDECIN : Dr. RACHID CONSTAT : LEGION CAN CERIGENE SECONDAIR PRESCRIPTION : XXXX RDV : 10/NOV/2007 HEURE : 10H30
<b>JPEG Compression Watermarked Image</b>	<b>Noised image</b> 	<b>Noised image</b> 	<b>Noised image</b> 
	<b>Detected Watermark Image</b>	PATIENTE : AMINA AGE : 51 ANS MEDECIN : Dr. RACHID CONSTAT : LEGION CAN CERIGENE SECONDAIR PRESCRIPTION : XXXX RDV : 10/NOV/2007 HEURE : 10H30	PATIENTE : AMINA AGE : 51 ANS MEDECIN : Dr. RACHID CONSTAT : LEGION CAN CERIGENE SECONDAIR PRESCRIPTION : XXXX RDV : 10/NOV/2007 HEURE : 10H30

Figure 12. Test image under sharpen attack ( DWT, R.DWT and CWT)

	<b>Noised image</b> 	<b>Noised image</b> 	<b>Noised image</b> 
	<b>PATIENTE : AMINA AGE : 51 ANS MEDECIN : Dr. RACHID CONSTAT : LEGION CAN CERIGENE SECONDAIR PRESCRIPTION : XXXX RDV : 10/NOV/2007 HEURE : 10H30</b>	<b>PATIENTE : AMINA AGE : 51 ANS MEDECIN : Dr. RACHID CONSTAT : LEGION CAN CERIGENE SECONDAIR PRESCRIPTION : XXXX RDV : 10/NOV/2007 HEURE : 10H30</b>	<b>PATIENTE : AMINA AGE : 51 ANS MEDECIN : Dr. RACHID CONSTAT : LEGION CAN CERIGENE SECONDAIR PRESCRIPTION : XXXX RDV : 10/NOV/2007 HEURE : 10H30</b>

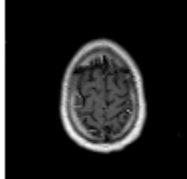
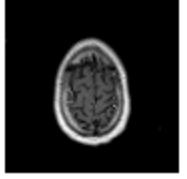
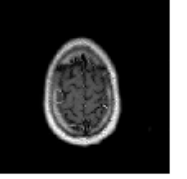
	<b>Watermarked image</b> 	<b>Watermarked image</b> 	<b>Watermarked image</b> 
	<b>PATIENTE : AMINA AGE : 51 ANS MEDECIN : Dr. RACHID CONSTAT : LEGION CAN CERIGENE SECONDAIR PRESCRIPTION : XXXX RDV : 10/NOV/2007 HEURE : 10H30</b>	<b>PATIENTE : AMINA AGE : 51 ANS MEDECIN : Dr. RACHID CONSTAT : LEGION CAN CERIGENE SECONDAIR PRESCRIPTION : XXXX RDV : 10/NOV/2007 HEURE : 10H30</b>	<b>PATIENTE : AMINA AGE : 51 ANS MEDECIN : Dr. RACHID CONSTAT : LEGION CAN CERIGENE SECONDAIR PRESCRIPTION : XXXX RDV : 10/NOV/2007 HEURE : 10H30</b>

Figure13. Test image under median filter attack (DWT, R.DWT and CWT)

For the images attack of Gamma correction, watermark can be recovered, in increasing the value greater than 0.5, both Axial image is recovered with real DWT and CWT.

The Table 2 and 3 illustrate that compared to other decompositions, the CWT, leads to better results quality, followed by real-DWT.; also showing a great effectiveness in removing the noise, at the stage of extracted.

Considering, Histogram equalization attack ,we found a slight improvement in contrast with an artificial increase in the clarity of the image and an equipartition of intensity, but some information is lost ,on the other side, watermark information failed to extracted for the images rotate 20°,30° in DWT and Real case; in CWT case the watermark information is correctly recovered without any error.

The data obtained from the tables can be connected with the data in Figures, which shows the most important findings.

In additional for the test result, it shows the following observation:

WAVELET TYPE	IMAGE CORONAL		IMAGE AXIAL	
	PSNR (indB)	SIM	PSNR	SIM
DWT	32.0999	0.968	32.1017	0.938
Real DWT	32.3009	0.979	32.1041	0.987
CWT	<b>32.9446</b>	<b>0.986</b>	<b>32.2623</b>	<b>0.989</b>

Table 1. PSNRs value and correlation (SIM) between original and watermarked images (no attack)

IMAGE CORONAL	DWT			Real DWT			CWT			
	ATTACK	PSNR1 (in dB)	SIM	PSNR2	PSNR1	SIM	PSNR2	PSNR1	SIM	PSNR2
Median Filter 3 X 3		29.312	0.918	30.123	31.204	0.895	31.987	32.014	0.909	32.987
JPEG 90%		31.966	0.927	32.910	32.987	0.942	33.125	33.9645	0.932	34.124
Gamma correctio 0.5		28.994	0.912	29.967	30.125	0.978	30.9142	31.8358	0.9155	31.785
Rotation 10°		17.120	0.691	20.959	29.896	0.891	30.998	31.1236	0.945	32.104
Histogram Equalization		29.193	0.915	30.102	31.258	0.921	32.154	31.8963	0.901	32.891
Sarpen		30.542	0.911	31.425	32.458	0.954	32.9689	33.2546	0.923	33.987

Table 2. PSNRs values between original and watermarked images and SIM between extracted and host watermark

IMAGE CORONAL	DWT			Real DWT			CWT			
	ATTACK	PSNR1 (in dB)	SIM	PSNR2	PSNR1	SIM	PSNR2	PSNR1	SIM	PSNR2
Median Filter 3 X 3		31.6426	0.912	31.967	32.655	0.899	32.9123	33.154	0.986	33.987
JPEG 90%		31.9696	0.9278	32.421	32.714	0.912	32.991	33.946	0.975	34.102
Gamma correctio 0.5		29.9945	0.902	30.123	30.725	0.988	30.9110	30.995	0.969	31.568
Rotation 10°		17.1007	0.631	26.567	29.996	0.881	30.1223	31.723	0.962	32.879
Histogram Equalization		29.152	0.895	30.127	31.356	0.901	30.987	31.996	0.928	32.564
Sarpen		29.1090	0.901	30.1879	31.6649	0.924	31.988	32.108	0.968	32.991

Table 3. PSNRs values between original and watermarked images and SIM between extracted and host watermark

- An observer had challenged images of coronal sequences with DWT.
- Axial images were considered acceptable for diagnosis by all observers for all wavelet transforms.

In case where the original image is revealed, we have the following result:

- Axial : 75% of observers found no significant loss of diagnostic information with RDWT and CWT ; an observer judged the images DWT too degraded to be reliable with the geometric attacks.
- Coronal: an observer has seen a marked image with DWT a limit the loss of information recorded 5.

## 7. Conclusion

In this study , has been proposed a new watermarking scheme, using different approach of wavelet transform, classical (DWT) and dual tree transform (DT-CWT), using real and complex version; combined with Bivariate Shrinkage function, this method exploits the benefits of Dual Tree Wavelet Transform propriety, it satisfies the security of watermark information and allows sharing the medical information remotely and manageably without storage space and without any affecter the medical image quality.

The Bivariate function is applying , for estimating the image at the extracted watermark step, the visual quality of medical images has been examined , after applying some attacks with PSNR (in dB), and SIM for testing the robustness for the scheme.

Considering the experimental results for DWT, real DWT and CWT , with images are decomposed it shown generally that our approach offer the flexible robustness, specially for CWT and real DWT and some results show again the parfait irreversibility.

We experienced the limitations of the mathematical approaches used similarity and PSNR, for same images.

However, sometimes a watermarked or extracted watermark images with high PSNR value does not have satisfactory visual quality for based one respondent to the test, the explanation is simple for this purpose; the transparency notion is related to the visibility of artifact introduced during the watermarking process. A watermarking procedure is described loyal if no visual difference can be seen between initial data and watermarked. However it is known whether the quality of the artifacts do not interfere with a human observer.

We can conclude that our method can be described as Semi-fragile, its reversibility and has flexible robustness, because the game of compromise robustness and invisibility ability is not only related to the wavelet quality but also to the construction technique of watermarking technique.

In the future we will try to enhance our algorithm in order to obtain watermarked medical images with less degradation and to have recovered watermark with better accuracy.

## References

- [1] Teddy Furon. (2002). Application du tatouage numérique à la protection de copie, these de l'Ecole nationale Supérieure des télécommunications.
- [2] Chang, M-C., Lou, D. C., Tso, H-K. (2007). Combined watermarking and fingerprinting technologies for digital image copyright protection, *The Imaging Science Journal*, V. 5.
- [3] Kingsbury, N. G. (1998). The dual-tree complex wavelet transform :a new technique for shift invariance and directional filter, *In: Proceedings IEE Digital Signal Processing Workshop*, n°86, Bryce canyon, UT, USA, Aug.9-12.
- [4] Mallat. (1998). A wavelet tour of signal processing, San Diego, CA, USA : Academic Press.
- [5] Kinsbury, N. G. (2000). A dual-tree complex wavelet transform with improved orthogonality and symmetry proprieties, *In: Proceedings of the IEEE Intl.Conf. on Image processing (ICIP)*.
- [6] Guo, H. (1995). Theory and applications of shift-invariant,time-varying and undecimated wavelet transform, MS thesis, Rice University.



- [7] Kinsbury, N.G. *Image processing with complex wavelets*. Phil.Trans. Royal Society London,( 1999).
- [8] Kinsbury, N.G. (2000). *A dual-tree complex wavelet transform with improved orthogonality and symmetry proprieties*. In: Proceedings of the IEEE Intl. Conf. on Image Proc.(ICIP).
- [9] Selesnick, I., Baraniuk, R. G., Kingsbury, N. G. (2005). *The dual-tree complex wavelet transform: IEE Signal Processing Magazine*, 22 (6) 123-151.
- [10] Selesnick, I., Li, K.(2003). *video denoising using 2D and 3D dual-tree complex wavelet transforms*: in wavelet applications in signal and image processing X(proc.SPIE 5207).
- [11] Lavent Sendur and Ivan Selesnick :*Bivariate Shrinkage With Local Variance Estimation: IEEE SIGNAL PROCESSING LETTERS*,DECEMBER (2002), 9 (12).
- [12] Puech, W., Michel DUMAS, Jean claude BORIE et MAGALIE Puech. (2001). Tatouage d'images cryptées pour l'aide au télédiagnostic, GRETIS ,GROUPE D'ETUDES DU TRAITEMENT DU SIGNAL ET IMAGES.
- [13] Giakoumaki, A. (2003). Paulopoulos and al, A Medical image watermarking scheme base on wavelet transform, *In: Engineering in Medecine and biology society*, Proceedings of the 25<sup>th</sup> Annual Intrenational Conference of the IEE.
- [14] Mostafa Salwa, A. K, Naser el-Sheiny and al.(2010). wavelet packets- based blind watermarking of medical image management, *Open Bio Med Eng.J.* 4, 93-98.
- [15] Golpira, H, Danyali, H. (2009). A blind reversible watermarking based on histogram shifting for medical image, *Signal processing and information Technology (ISSPIT)*, IEEE.
- [16] Chen-Ri Piao, Dond-Min andal. (2008). Medical Image Authencation Using hash Function and Integer wavelet Transform, *Image and Signal Processing*, Congress, on 1, 7-10.
- [17] Chokri Chemak and al., (2007). New watermarking Scheme for security and transmission of medical images for packetNeuro project, *Radio Engineering*, 4. Dec.
- [18] Loo, P., Kingsbury, N, G. (2000). Digital watermarking using complex wavelet's, *In: Proc. ICIP2000*, Vancouver, Sept.
- [19] Mabtoul, S., Elhaj, E. H. I., Aboutajdine, D. (2008). A Robust Digital Image Watermarking Method Using Dual Tree Complex Wavelet Transform, *IEEE Symp. On Communication (ISCC 2008)*, p. 1000-1004.
- [20] Plantz, B., Maeder, A. (2005). Medical Image watermarking: A study on image degradation, *Proc. Of the Australian pattern recognition Society (APRS) workshop on Digital Image computing (WDIC 2005)* p. 3-8.
- [21] Peter Meerwald. (2011). *Digital Image in the wavelet transform domain*, salzburg, am11, Janner, these.
- [22] Sendur, L., Selesnick, I. W. (2002). Bivariate shrinkage functions for wavelet-based denoising exploiting interscale dependence. *IEEE Trans. on Signal Processing.* 50 (11) 2744-2756, November.